Short-range Correlations in a CBF description of closed-shell nuclei.*

F.Arias de Saavedra [1], G.Co' [3], A.Fabrocini [4],
S.Fantoni [5], I.E.Lagaris [2], A.M.Lallena [1]

1) Departamento de Fisica Moderna, Universidad de Granada,
Granada, *Spain*
2) Department of Physics, University of Ioannina,
Ioannina, *Greece*
3) Dipartimento di Fisica, Università di Lecce and
INFN, Sezione di Lecce,
Lecce, *Italy*
4) Dipartimento di Fisica, Università di Pisa and
INFN, Sezione di Pisa,
Pisa, *Italy*
5) Interdisciplinary Laboratory for Advanced Studies (ILAS) and
INFN, Sezione di Trieste,
Trieste, *Italy*

Abstract

The Correlated Basis Function theory (CBF) provides a theoretical framework to treat on the same ground mean–field and short–range correlations. We present, in this report, some recent results obtained using the CBF to describe the ground state properties of finite nuclear systems. Furthermore we show some results for the excited state obtained with a simplified model based on the CBF theory

*Presented by G.Co' at the Second Workshop on Electromagnetically Induced Two–Nucleon Knockout, Gent, May 17–20, 1995.

1 Introduction

In the description of a many–body system, the word **correlation** indicates the fact that the state of each particle of the system depends on the presence of the other particles.

In an infinite system of interacting particles, this definition of correlation can be exactly translated saying that *anything beyond the Fermi–gas model is a correlation.* For a finite set of particles the phrase *anything beyond the shell model is a correlation*, does not translate the definition of correlation given above since the mean–filed is already correlating the particles of the system, localising their presence around a specific point of the space.

A proper description of a finite many–body system should treat on the same ground the correlation generated by the mean–field and those produced by the residual interaction among the particles.

The Correlated Basis Function theory (CBF) provides a theoretical framework for this consistent treatment. The CBF has been applied successfully to both few–body systems and nuclear matter (for a review see ref. [1]).

In recent years, we have started a work aimed to apply the CBF to the description of medium and heavy nuclei [3, 4]. In this report we shall present some recent results of this work.

2 CBF and FHNC theories

The CBF is based upon the variational principle

$$\delta E[\Psi] = \delta \frac{< \Psi | H | \Psi >}{< \Psi | \Psi >} = 0, \tag{1}$$

which corresponds exactly to the Schrödinger equation if the variation is performed considering the full Hilbert space of many–body wave functions, or in other words, if no limitations on the structure of the many–body wave function $|\Psi >$ are enforced.

On the other hand, one solves the variational principle instead of the Schrödinger equation because one wants to work in a limited sub–space of the Hilbert space. For example, the assumption that $|\Psi >$ is a Slater determinant of single particle wave functions leads to the Hartree–Fock equations.

The assumption on the structure of $|\Psi >$ used in the CBF is:

$$\Psi(1,2,...,A) = F(1,2,...,A)\Phi(1,2,...,A) \tag{2}$$

where Φ is a Slater determinant and F is a many–body correlation function defined as a symmetrized product of two-body correlation functions:

$$F(1,...,A) = \mathcal{S} \prod_{i<j} [\sum_{n=1}^{M} f^{(n)}(r_{ij}) O^{(n)}(i,j)] \tag{3}$$

In the above equation $\mathcal{S}$ represents the symmetrizer operator and the two–body correlation functions have been expressed in a most general form, where the state dependence, given by the operators O^n, is, in general, the same of the hamiltonian [2]. This correlation operator contains only explicit two–body correlations. More general forms, mainly used in light nuclei, may also include three–body correlations.

The variational procedure consists in performing the variation on the correlation function and on the set of single particle wave functions in order to find the minimum of the energy functional of eq. 1. This requires the evaluation of complicated multidimensional integrals. The most direct approach to tackle the problem is the numerical evaluation performed with Monte Carlo technology. In this case the full procedure is called Variational Monte Carlo (VMC) calculation. This brute force method is, unfortunately, not suitable to describe medium and heavy nuclei since the number of spin–isospin states to be sampled becomes enormous (for the ^{40}Ca nucleus is of the order of the Avogadro number).

Since we are interested in the description of medium and heavy nuclei we used a different technique: the cluster expansion. This technique is better illustrated when the correlation function is purely scalar and commutes with the nuclear potential, V. In this case the mean value of V can be written as:

$$< \Psi|V|\Psi >=< \Phi|FVF|\Phi >=< \Phi|VF^2|\Phi >=< \Phi|V\prod_{i<j}^{A}(f^2(r_{ij}))|\Phi > \qquad (4)$$

where r_{ij} represents the distance between the i and j nucleons. The last equality of the previous equation follows from the orthonormality of the single particle wave functions. We definine a function h as:

$$f^2(r) = 1 + h(r). \qquad (5)$$

The importance of this function lies in the fact that it is appreciably different from zero only in a small region of r, and it can be used as an expansion parameter. The mean value of the potential becomes:

$$\begin{aligned} &< \Psi|V|\Psi >=< \Phi|V\prod_{i<j}^{A}(1+h(r_{ij}))|\Phi > \\ = \quad &< \Phi|V(1+h(r_{12}))(1+h(r_{13}))...(1+h(r_{23}))...|\Phi > . \end{aligned} \qquad (6)$$

The cluster structure clearly shows up in the above equation.

Let's consider the term obtained retaining only the 1's in the expansion of F^2. We obtain:

$$< \Phi|V|\Phi > \qquad (7)$$

which is the mean value of the potential between the uncorrelated states. If V is a two–body potential

$$V = \frac{1}{2}\sum_{i<j}^{A} v(r_{ij}), \qquad (8)$$

the sum of all the terms linear in h generates two–body cluster diagrams

$$\frac{A(A-1)}{2} < \Phi|v(r_{12})h(r_{12})|\Phi >, \qquad (9)$$

and three– or four–body cluster diagrams of the form:

$$\frac{A(A-1)}{2} < \Phi|v(r_{12})\sum_{i<j}^{A} h(r_{ij})|\Phi > . \qquad (10)$$

The three–body diagrams are obtained when either i or j is equal to 1 or 2 and the other index is different, while in the four–body diagrams both i and j are different from 1 and 2. Summing all the terms quadratic in the h functions,

$$< \Phi|V\sum h(r_{ij})h(r_{lm})|\Phi >, \qquad (11)$$

three–, four–, five– and six–body cluster diagrams are obtained.

The procedure continues considering all the terms given by eq. 6. A similar expansion can be derived for the kinetic energy mean value.

The analysis of the cluster expansion is done in a more efficient way using the so–called Mayer diagrams [5]. From this analysis it turns out that the mean value of the hamiltonian between the two correlated states can be expressed simply in terms of two classes of diagrams: the nodal diagrams and the elementary, or bridge, diagrams (see references [2, 6, 7] for more details).

The Fermi Hypernetted Chain (FHNC) provides a set of integral equations which allows one to sum up all the nodal diagrams. There is not closed form to do the same for the elementary diagrams. They should be calculated one by one like in ordinary perturbation theories.

A usual approximation in this kind of calculations, the so–called FHNC/0 approximation, consists in neglecting the elementary diagrams. It is worth to stress here that the FHNC/0 calculations differ from the Monte Carlo ones only by the fact that the elementary diagrams are not considered. The relevance of these diagrams has been studied in nuclear matter where it has been found that their contribution to the energy is small [1, 2, 8]. This is not the case for other many-body systems, like liquid helium [9].

Our first goal was to test the validity of FHNC theory against VMC calculations [10]. For this reason we have performed calculations in model nuclei using scalar correlation functions and semi-realistic interactions. Our model nuclei are composed by protons and neutrons having the same radial single–particle wave functions, their angular momentum coupling is done in the $l-s$ scheme, and the Coulomb interaction is switched off.

The comparison between our results and the VMC ones are presented in tab.1 where, in addition to the binding energies $< E >$, the contribution of the Majorana $< v_M >$ and Wigner $< v_W >$ terms of the potential and that of the kinetic energy $< T >$ are shown.

The calculations have been performed using the Brink and Boeker B1 interaction [11] and with harmonic oscillator single particle wave functions.

The FHNC results are presented in the rows labelled FHNC/0. We observe the fact that in ^{16}O the binding energies differ from the VMC results by a factor of about the 10%. More important was the fact that the spin sum rule,

$$S_\sigma = \frac{1}{3A}\int d^3r_1 d_2^3 < \Psi | \sum_{i\neq j} \delta(\mathbf{r_1}-\mathbf{r_i})\delta(\mathbf{r_2}-\mathbf{r_j})\boldsymbol{\sigma}_i\cdot\boldsymbol{\sigma}_j|\Psi >= -1, \qquad (12)$$

which should hold for the spin saturated systems we have studied, was not satisfied by a 10% factor.

Since the only difference between FHNC/0 and VMC calculations is the absence in the former calculations of the elementary diagrams, we attributed to them the discrepancy between the two results. For this reason we have performed other calculations inserting the lowest order elementary diagram. The results of these calculations are presented in tab.1 by the rows labelled as FHNC-1. We found that the inclusion of the elementary diagram was practically affecting only the Majorana part of the potential energy, and therefore we expected big changes in the spin sum rule. In effect the spin sum rule resulted to be satisfied at the 1% level.

These results, in spite of the importance of some classes of elementary diagrams, gave us confidence about the validity of our approach.

The next step of our work consisted in applying the formalism to real nuclei, with different radial wave functions for protons and neutrons, angular momentum coupling in a $j-j$ scheme, and with Coulomb interaction. In this new situation we found that the

$j-j$ coupling is generating, in the nuclei with unsaturated l levels, a new statistical correlation.

In tab.2. we present the results of calculations performed keeping fixed the Woods-Saxon mean–field which generates the single particle wave functions and changing the correlation function in order to minimise the binding energy. The interaction used is the S3 force of Afnan and Tang [12] extended to consider the odd channels as described in ref. [3].

The results of the column $F1$ have been obtained using the same mean–field potential for protons and neutrons (a Woods-Saxon well without spin–orbit term), switching off the Coulomb interaction and the new statistical correlation. The effect of this new correlation can be seen comparing the results of column $F1$ with those column $F2$. The only difference with the calculation of the $F1$ column is just the inclusion of the new correlation terms. The effect of this new correlation is present only in the potential energy term of the ^{12}C, ^{48}Ca and ^{208}Pb nuclei which have some unsaturated l shell, and it is rather small.

The $F3$ column presents the results obtained adding the Coulomb interaction in the hamiltonian. The contribution of the nuclear interaction (V) to the binding energy is about the same for ^{40}Ca, ^{48}Ca and ^{208}Pb. This nuclei are sufficiently large to allow the nuclear interaction to *saturate*. On the other hand, the contribution of the Coulomb interaction (V_c), because of the infinite range of the force, increases like the number of the protons pairs.

The $F4$ column shows the results obtained inserting the Coulomb potential also in the mean–field. We have used the potential generated by a homogeneously charged sphere. Other choices did not make any relevant difference.

Instead of performing a full minimisation of the energy functional changing both the mean–field and the correlation function, we took from the literature Woods–Saxon potentials fixed in order to reproduce single particle energies around the Fermi surface, and with these mean–fields we minimised the binding energies finding the optimal correlation functions for both the B1 and S3 interactions. The results of these calculations are presented in tab.3 and they show the same characteristics of those of tab.2. The nuclear interaction *saturates* for the heavier nuclei while the contribution of the Coulomb interaction increases with the number of protons.

It is interesting to compare the results obtained by the FHNC/0 calculations (rows E) with those obtained including the elementary diagram (rows $E/4$). The contribution of the elementary diagram is noticeable in the lighter nuclei. In ^{12}C is of the order of the 10% and even more. As soon as the number of particles increases, the elementary diagram becomes less important. In ^{208}Pb its contribution is of few parts on a thousand. This fact is in agreement with our experience of nuclear matter calculations where the elementary diagrams are irrelevant.

An interesting feature of these calculations is shown in fig.1 where the optimal correlation functions are shown. The correlation functions seem to depend only from the interaction and not from the mean–field. The correlation functions obtained with the $S3$ interaction have deeper minima than those obtained with the $B1$ interaction.

In fig.2 we compare the uncorrelated proton distribution (full lines) with those calculated with our theory using the $B1$ and $S3$ interactions (dashed and dashed dotted lines respectively). The effect of the correlation on the distributions seems to be larger for the calculations done with the $B1$ interaction than in the case of the $S3$ interaction. It is remarkable the small effect shown on the ^{208}Pb distribution. We found analogous effects on the neutrons distributions.

In fig.3 we show the proton momentum distributions. In this figure the presence of

short–range correlations shows up at high momentum value where the FHNC results are orders of magnitude bigger than the uncorrelated results. The differences between the calculations performed with the two interactions are small if compared with those with the uncorrelated momentum distribution.

3 The model

The CBF-FHNC theory presented above is a good approximation for the exact solution of the many-body Schrödinger equation. A CBF basis may also be constructed, to be used in perturbation theory. This expansion is expected to have a fast convergence, since much of the non–perturbative physics, related to the short-range part of the nuclear potential, is already embedded in the basis itself.

Unfortunately it is unrealistic to expect of being able to calculate in a short time the two-nucleon emission cross sections using this theory. The comparison with the experimental data produced in the next few years by the electron accelerators will be done through models. This theory is however a basis and/or a testing ground for these models.

It is in this perspective that we have started to develop a simplified model of the theory. This model consists essentially in calculating only the cluster expansion terms with a single dynamical correlation line. The nice feature of this model is that, in spite of the relative simplicity with respect to the full theory, it satisfies the same set of sum rules of the full calculation. Details of the model can be found in ref. [13].

In fig.4 we compare the proton density distribution obtained with our model (dotted line), with that obtained performing the full FHNC calculation (dashed line). The model is slightly emphasising the effect of the correlations.

The relative simplicity of the model allows us to include easily the effect of the state dependent part of the correlation which are shown in fig.5. In this figure the full line is the uncorrelated proton distribution and the other lines have been obtained including the various state dependent channels. The number from 1 to 4 are indicating the inclusion of each central channel $(1, \boldsymbol{\sigma}_i \cdot \boldsymbol{\sigma}_j, \boldsymbol{\tau}_i \cdot \boldsymbol{\tau}_j, \boldsymbol{\sigma}_i \cdot \boldsymbol{\sigma}_j \boldsymbol{\tau}_i \cdot \boldsymbol{\tau}_j)$ and the 5 and 6 the isoscalar and isovector tensor channels[14]. The lower panel shows the difference between uncorrelated and correlated distributions.

We have recently extended our model to describe excited states. In fig.6 we present the charge form factors for the discrete transitions $1f_{7/2} - 2s1/2^{-1}$ in ^{40}Ca and ^{48}Ca. The dashed lines show the results obtained with the uncorrelated shell model, and the full lines the results obtained with our model.

4 Conclusions

Electron scattering experiments have, so far, investigated the one-body part of the nuclear many-body wave function. With the double coincidence experiments we shall start to investigate the two-body part of the nuclear wave function. The mean–field models, quite successful in describing the one–body observables, are inadequate to describe two-body properties of the nuclei. A profitable comparison between theory and experiment cannot be obtained adding corrections to mean–field models fixed to reproduce one–body properties. This because in these models, part of the effects we want to investigate, those of the correlation, are already taken into account in an average way.

A proper theoretical description of the nuclear two-body properties can be obtained only if one treats on the same ground mean-field, correlations and also final state interac-

tions. The CBF-FHNC theory provides a theoretical framework to carry on this ambitious program. The theory is technically extremely involved and we believe it is necessary to develop simpler models to describe the forthcoming experimental data. The CBF–FHNC theory can be used as a starting point or testing ground for these models which should be developed.

References

[1] V.R.Pandharipande, "Proceedings of Cargese summer School 1989", J. Tran Tranh Van and J. Negele Ed.s (Plenum Press, NY 1990).

[2] V.Pandharipande and R.B.Wiringa, Rev. Mod. Phys. 51 (1979) 821.

[3] G.Co', A.Fabrocini, S.Fantoni and I.Lagaris, Nucl. Phys. A549 (1992) 439.

[4] G.Co', A.Fabrocini and S.Fantoni, Nucl. Phys. A568 (1994) 73.

[5] J.Mayer and M.Mayer, Statistical Mechanics, New York, Wiley 1940.

[6] S.Rosati, Proc. Int. School of Physics E. Fermi, Course LXXIX, Varenna, A. Molinari editor, North Holland, Amsterdam, (1981) 73.

[7] A.Fabrocini and S.Fantoni, First International Course of Condensed Matter, D.Prosperi, S.Rosati and G.Violini eds., Bogota', World Scientific (1986) 87.

[8] R.B.Wiringa, private communication

[9] F.Arias de Saavedra, Ph. D. Thesis, Granada 1992, unpublished.

[10] E.Buendìa private communication

[11] D.M.Brink and E. Boecker, Nucl. Phys. A91 (1967) 1.

[12] I.R.Afnan and Y.C.Tang, Phys. Rev. 175 (1968) 1337.

[13] G.Co', Nuov. Cim. A108 (1995) 623.

[14] R.B.Wiringa, V.Ficks and A.Fabrocini, Phys Rev. C38 (1988) 1010.

^4He	$< v_M >$	$< v_W >$	$< T >$	$< E >$
$FHNC/0$	-132.5	24.5	83.9	-44.5
$FHNC-1$	-125.6			-37.7
VMC	-123.8	24.8		-36.4
^{16}O	$< v_M >$	$< v_W >$	$< T >$	$< E >$
$FHNC/0$	-421.6	-63.3	329.8	-168.2
$FHNC-1$	-403.8			-150.4
VMC	-402.6	-62.3	327.1	-150.9

Tab. 1. Energies per nucleon, in MeV, for the ^4He and ^{16}O model nuclei.

^{12}C	F1	F2	F3	F4
V	-21.37	-21.22	-21.22	-21.03
V_C			0.64	0.63
T	19.23	19.23	19.23	19.04
E	-2.14	-1.99	-1.35	-1.36
^{16}O	F1	F2	F3	F4
V	-26.08		-26.08	-25.74
V_C			0.87	0.86
T	20.09		20.09	19.80
E	-5.99		-5.12	-5.08
^{40}Ca	F1	F2	F3	F4
V	-32.47		-32.47	-31.83
V_C			1.95	1.91
T	23.95		23.95	23.43
E	-8.52		-6.57	-6.49
^{48}Ca	F1	F2	F3	F4
V	-33.44	-33.40	-33.40	-32.60
V_C			1.62	1.55
T	26.11	26.11	26.11	25.49
E	-7.33	-7.29	-5.67	-5.54
^{208}Pb	F1	F2	F3	F4
V	-33.86	-33.84	-33.84	-32.96
V_C			3.97	3.83
T	24.69	24.69	24.69	24.14
E	-9.17	-9.15	-5.18	-4.98

Tab. 2. Energies per nucleon, in MeV, for the five nuclei considered.

B1	^{12}C	^{16}O	^{40}Ca	^{48}Ca	^{208}Pb
V	-24.00	-27.30	-33.20	-32.10	-34.283
V_C	0.67	0.86	1.90	1.56	3.819
T	19.69	17.95	20.90	21.18	20.862
E	-3.64	-8.49	-10.40	-9.36	-9.602
$E/4$	-3.18	-7.93	-9.74	-8.84	-9.586
S3	^{12}C	^{16}O	^{40}Ca	^{48}Ca	^{208}Pb
V	-24.18	-26.53	-32.37	-31.13	-31.360
V_C	0.68	0.88	1.95	1.59	3.824
T	22.34	20.69	24.14	24.18	22.673
E	-1.16	-4.96	-6.28	-5.36	-4.863
$E/4$	-1.04	-4.83	-6.17	-5.51	-4.856

Tab. 3. Energies per nucleon, in MeV, obtained with $B1$ and $S3$ interaction. The results labelled E have been obtained with a FHNC/0 calculation, while those labelled $E/4$ have been obtained including the elementary diagram.

Figure captions

Fig. 1. Correlation functions obtained in the calculations whose results are presented in Table 3.

Fig. 2. Proton density distributions. Full lines, mean–field, dashed and dashed–dotted lines, FHNC-1 calculations with $S3$ and $B1$ interaction, respectively.

Fig.3. Proton momentum distributions. Full lines, mean–field, dashed and dashed–dotted lines, FHNC-1 calculations with $S3$ and $B1$ interaction, respectively.

Fig. 4. Proton distribution calculated with the same gaussian correlation in FHNC (dashed line) and in the model described in the text (dotted line). The full line represents the mean–field density distribution.

Fig. 5. Proton distributions obtained with our model using state dependent correlations taken from nuclear matter[14]. The lower panel show the differences between the uncorrelated density distribution (full line in the upper panel) and the various correlated density distributions. The meaning of the various lines is given in the text.

Fig. 6. Charge form factor for the transition $(1f_{7/2} - 2s_{1/2}^{-1})$ in ^{40}Ca (left panel) and ^{48}Ca (right panel). The dashed lines represent the results obtained with the uncorrelated shell model while the full lines are showing the results obtained with our model.

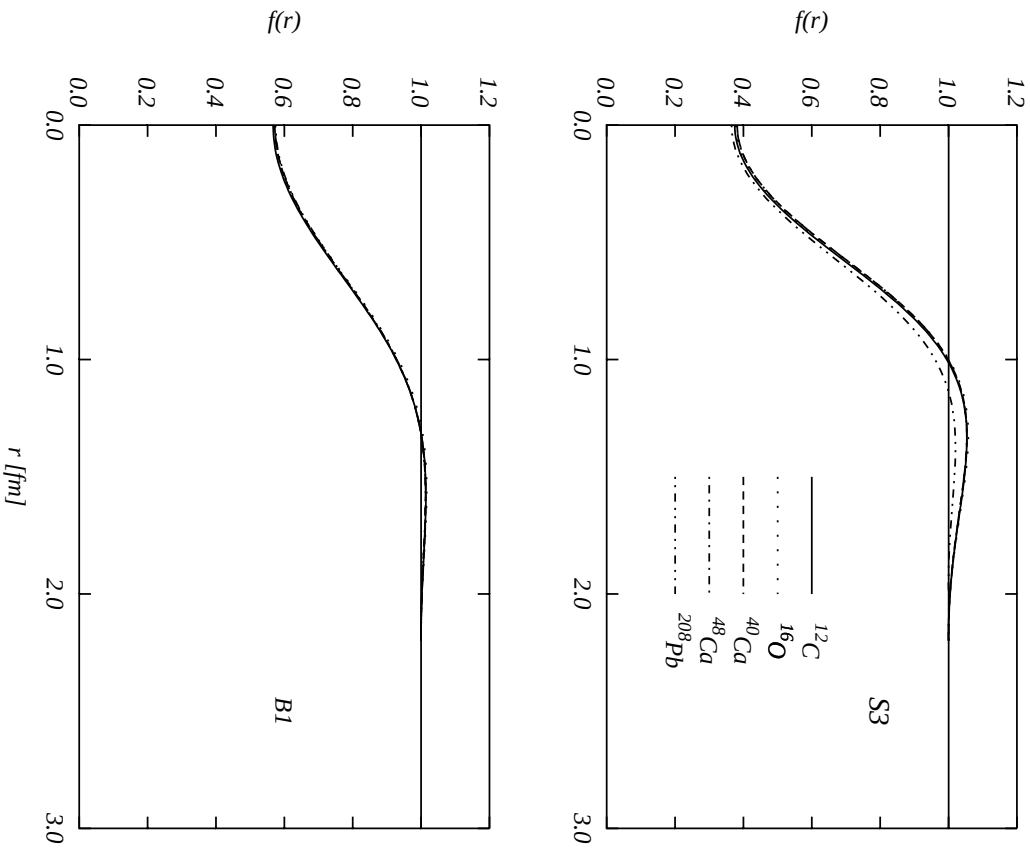

Figure 1:

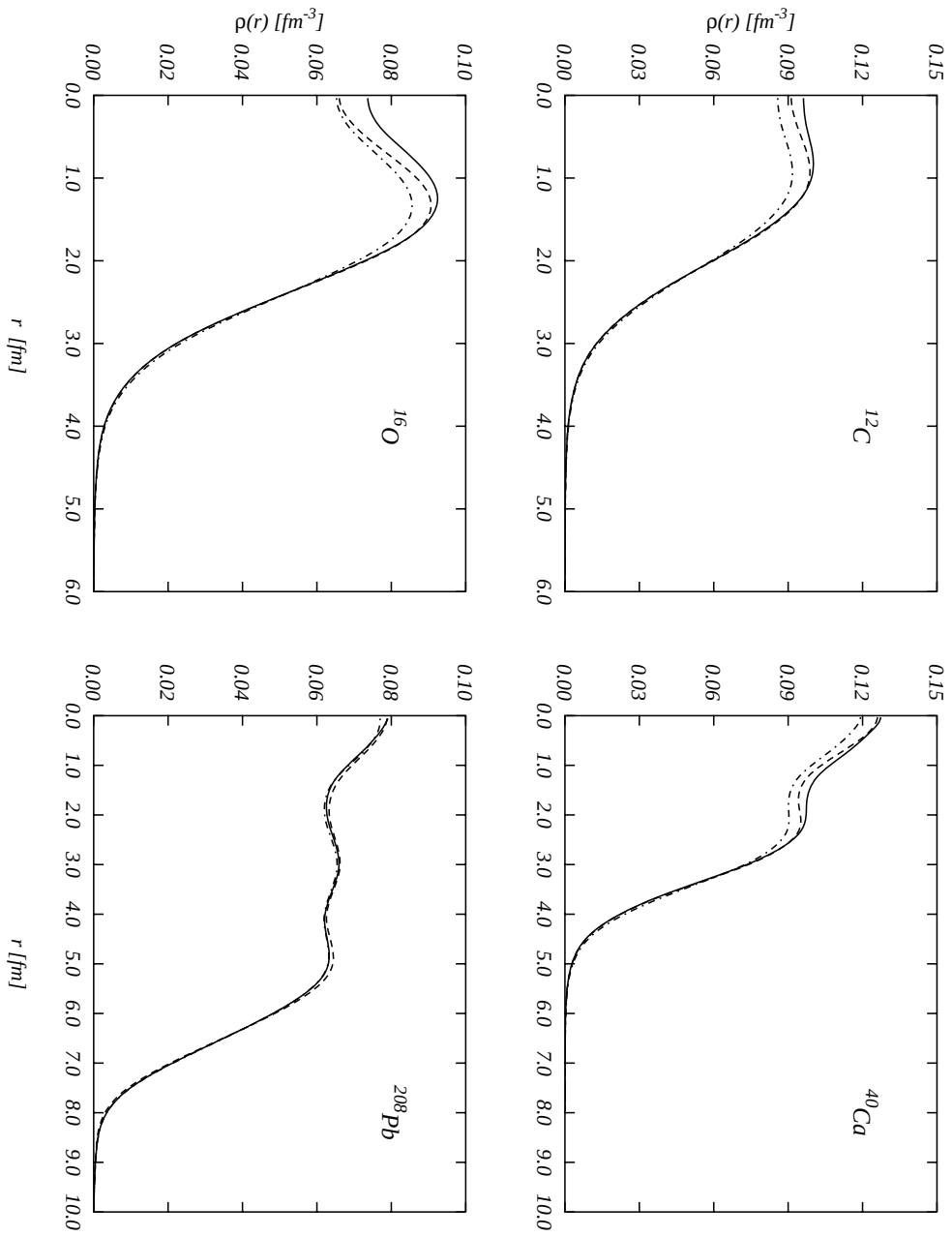

Figure 2:

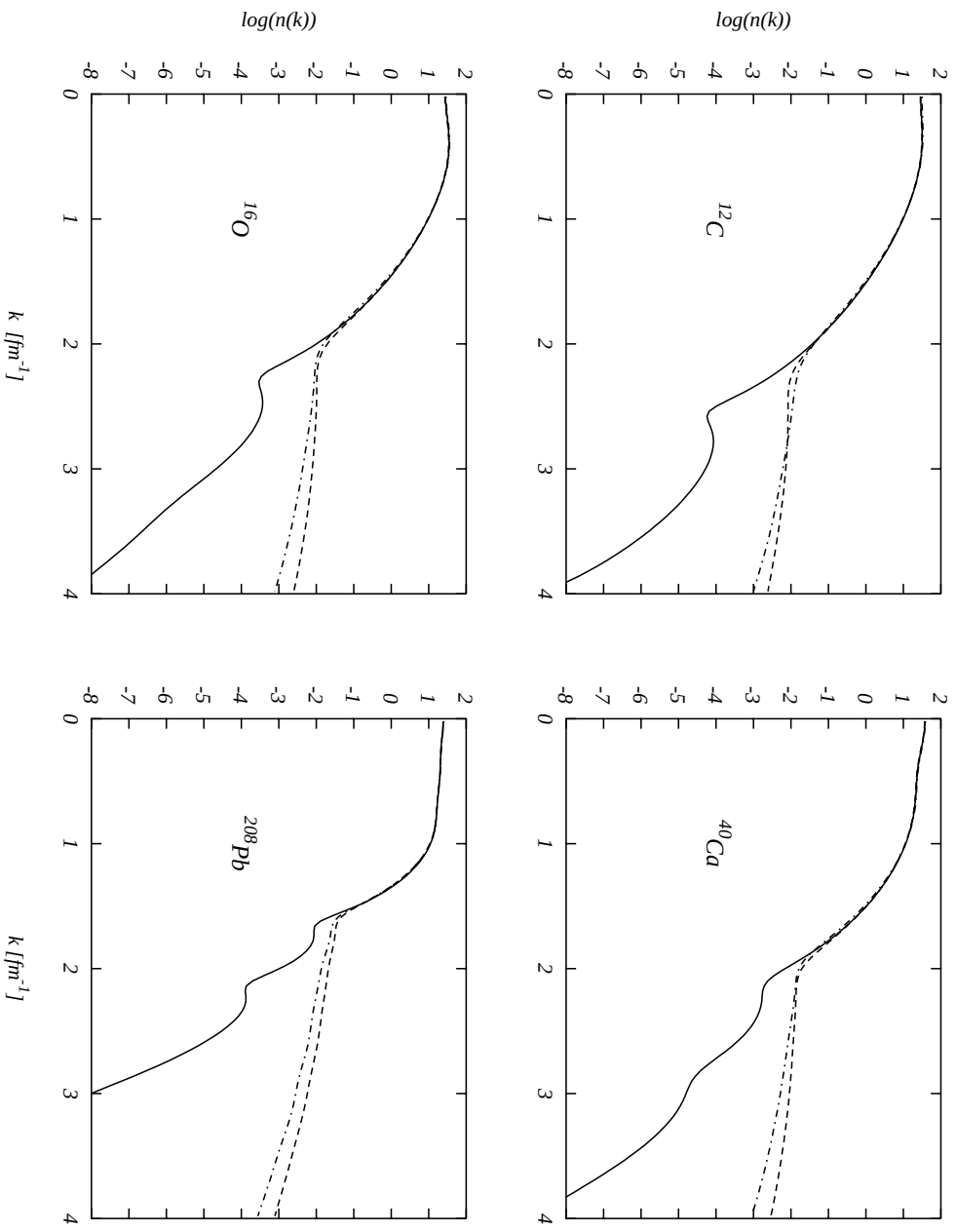

Figure 3:

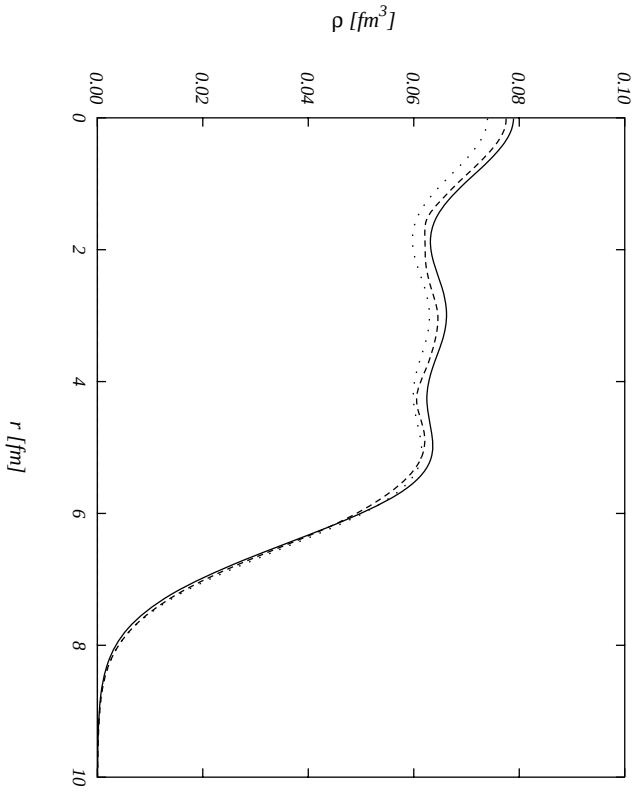

Figure 4:

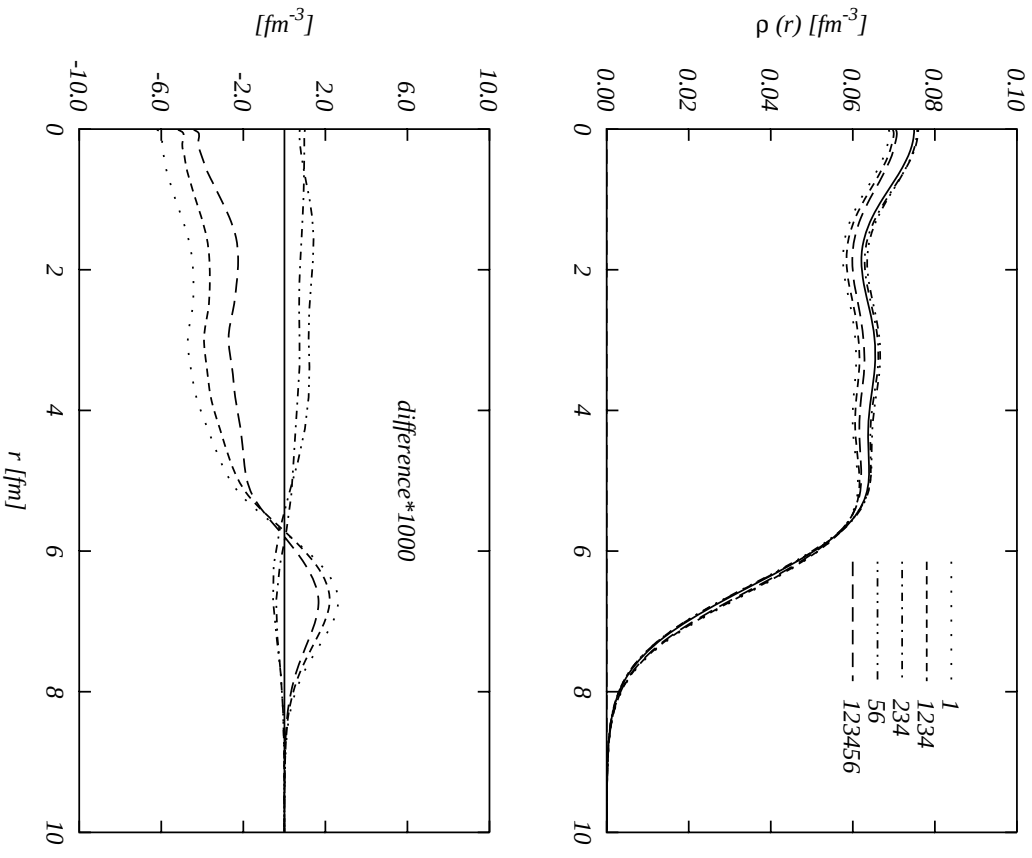
ρ (r) [fm-3]
0.10
0.08
0.06
0.04
0.02
0.00
0
2
4
6
8
10
1
1234
234
56
123456
[fm-3]
10.0
6.0
2.0
-2.0
-6.0
-10.0
difference*1000
r [fm]

Figure 5:

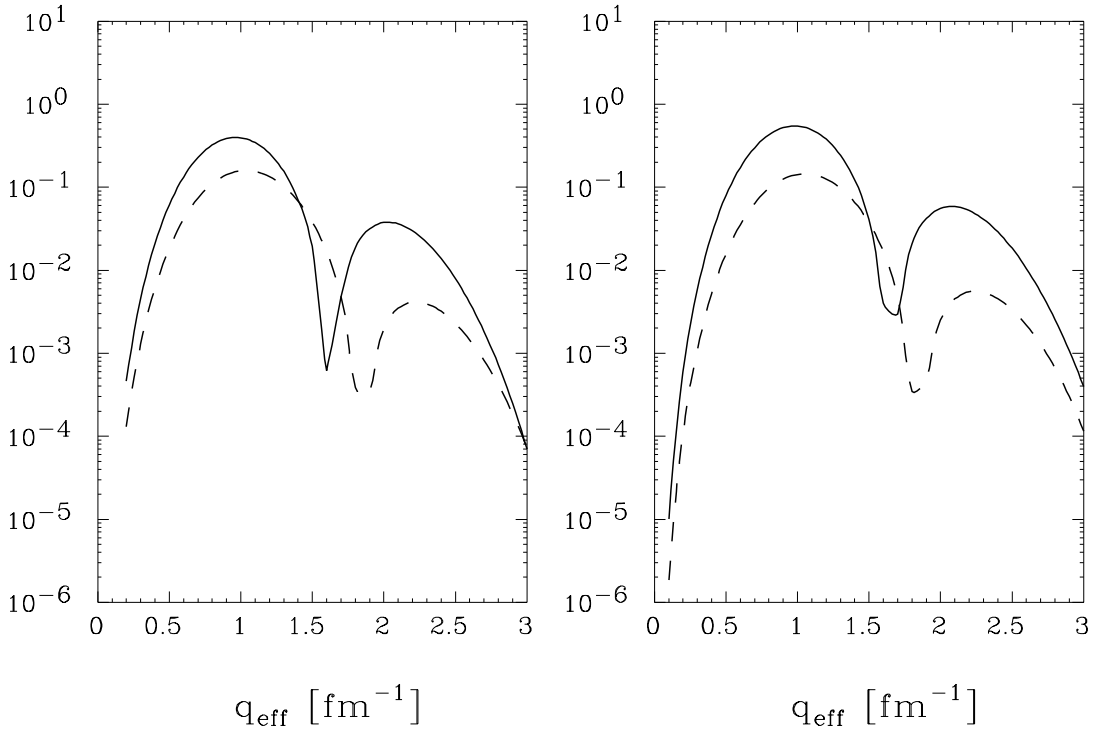

fig.6

Figure 6: